LBL-29588

Lawrence Berkeley Laboratory
UNIVERSITY OF CALIFORNIA

Materials & Chemical Sciences Division

Presented at the Applied Superconductivity
Conference, Aspen, CO, September 24–28, 1990,
and to be published in the Proceedings

The Effect of the Quantum Susceptance on the Gain of Superconducting Quasiparticle Mixers

C.A. Mears, Q. Hu, and P.L. Richards

September 1990

Prepared for the U.S. Department of Energy under Contract Number DE-AC03-76SF00098.

LBL-29588

The Effect of the Quantum Susceptance on the Gain of Superconducting Quasiparticle Mixers*

C. A. Mears, Qing Hu[a)] and P. L. Richards
Department of Physics , University of California at Berkeley, and
Materials and Chemical Sciences Division, Lawrence Berkeley
Laboratory, Berkeley, CA 94720

[a)] Present address: Department of Electrical Engineering and Computer Science and Research Laboratory of Electronics, Massachusetts Institute of Technology, Cambridge, MA 02139

* This work was supported in part by the Director, Office of Energy Research, Office of Basic Energy Sciences, Materials Sciences Division of the U. S. Department of Energy under Contract No. DE-AC03-76-SF00098.

LBL-29588

THE EFFECT OF THE QUANTUM SUSCEPTANCE ON THE GAIN OF SUPERCONDUCTING QUASIPARTICLE MIXERS

C. A. Mears, Qing Hu[a] and P. L. Richards
Department of Physics, University of California at Berkeley, and
Materials and Chemical Sciences Division, Lawrence Berkeley Laboratory, Berkeley, CA
94720

Abstract

A detailed analysis of the effects of the quantum susceptance on the performance of superconductor-insulator-superconductor (SIS) mixers is performed. We find that the principal effects of the quantum susceptance is to change the dc bias at which optimum coupling of the signal to the mixer occurs, and to change the output admittance at the IF frequency, thus changing the available gain.

Introduction

Heterodyne receivers which use the nonlinear quasiparticle currents in SIS tunnel junctions have been shown to provide the lowest noise over at broad range of the millimeter and sub-millimeter electromagnetic spectrum.[1] The behavior of SIS tunnel junctions when used as mixers or video detectors is described by the Tucker[2-4] theory of quantum mixing.

The quasiparticle tunneling current exhibits both resistive (in-phase) and reactive (out-of-phase) response to an ac drive.[5] The contribution from the out-of-phase response only becomes important at frequencies $f \geq e\Delta V/h$, where ΔV is the voltage range of the nonlinearity near the sum-gap voltage, e is the charge on an electron, and h is Planck's constant. At such frequencies the quasiparticle response of SIS tunnel junctions must be treated quantum mechanically. We have recently reported a direct measurement of this reactive term in the small signal limit ($V_{RF} << hf/e$, where V_{RF} is the amplitude of the high frequency voltage drive) at millimeter wave frequencies.[6,7] Such out-of-phase currents are also predicted to exist when the junction is driven by a signal of moderate strength ($V_{RF} \approx hf/e$). The existence of such currents can be inferred by studying I-V curves of junctions pumped at this strength.[7,8]

When an SIS junction is used as a heterodyne mixer, the local oscillator (LO) is typically of this strength. The effect of out-of-phase quasiparticle currents on the operation of SIS mixers has been a controversial subject. In the earliest studies of quantum mixers, it was speculated that the nonlinear susceptance caused by out-of-phase currents would have a harmful effect analogous to that of the nonlinear capacitance in Schottky diodes. Subsequently, it was speculated that the conversion gain observed in SIS mixers is due to a parametric amplification from this susceptance. Feldman[9] later argued that the effect of the quantum susceptance is subtle and not responsible for the observed conversion gain. A later theoretical analysis by Feldman and Face[10] found the existence of quantum susceptance increased the range of signal and image embedding admittances which gave infinite available gain. They also argued that the quantum susceptance can be roughly expressed as a time delay in the quasiparticle response. It is undoubtably true that mixer calculations which use the full quantum theory of mixing correctly include all effects of the quantum susceptance. What has been missing is an intuitive understanding of the ways in which the quantum susceptance affects mixer gain.

To our knowledge, all previous detailed work is limited in that the analysis was carried out at a single dc bias voltage. The quantum susceptance is a rapidly changing function of the dc bias voltage. Therefore, any complete analysis must treat the dc bias voltage as a free parameter. In other words, the dc bias point that yields the best performance with a specific set of signal and image admittances may not be the optimum point for a different set of admittances. In this paper we present an analysis of the performance of a hypothetical mixer with typical parameters as a function of bias voltage. We argue that the principal effects of the quantum susceptance is to change dc bias voltage at which the optimum performance occurs, and to change the output admittance of the mixer at the IF frequency, thus changing the available gain.

Mixer Model

We wish to discuss the effect of the quantum susceptance on the performance of an SIS mixer under realistic experimental conditions. We therefore carry out our calculations for a hypothetical mixer operated under the following conditions. We assume a junction whose normal resistance is 100 Ω, with geometrical capacitance C = 65 fF, yielding $\omega R_N C = 4$ at $f = \omega/2\pi = 100$ GHz. The capacitance is assumed to be resonated by an inductive tuning element. The susceptance of this tuning element varies with frequency 3 times faster than a lumped inductor with the same value of susceptance. Such a frequency dependence can be achieved with low-impedance tuning stubs made from superconducting transmission lines.[11,12,13]. The real part of the imbedding admittance is assumed to be 0.02 Ω^{-1} at both side band frequencies as well as at the IF.

The dc I-V curve chosen for our hypothetical junction is shown in Fig. 1. This I-V curve was measured from a Nb/Al_2O_3/Nb junction fabricated using the tri-layer technique at NIST. The moderately sharp current rise at the sum-gap voltage is typical for this widely used junction technology. Our hypothetical mixer is similar to many mixers that have been built to operate in the mm-wave band, and is therefore useful for the discussion of the effects quantum susceptance has on the operation of actual receivers.

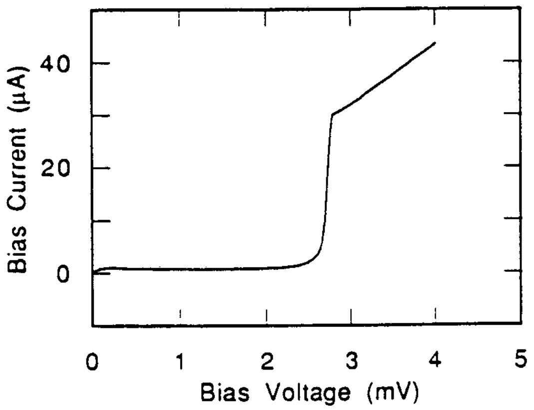

Fig. 1. The dc I-V curve used in the study

---

[a] Present address: Dept. of Electrical Engineering and Computer Science and Research Laboratory of Electronics, Massachusetts Institute of Technology, Cambridge, MA 02139

Manuscript received September 24, 1990

The Three-Port Model

All calculations presented in this paper were done using the 3-port model. In this model, we assume that tunneling currents at the first and higher harmonics of the local oscillator are shunted by the geometrical capacitance of the junction. This assumption is valid as long as the amplitude of the LO voltage drive is not so large that large currents flow at the first harmonic frequency where $\omega R_N C$ = 8.

We assume that the amplitude of the LO voltage drive V_{LO} is independent of bias voltage. This is unphysical because the large signal input admittance of the junction depends on the dc bias voltage, which causes V_{LO} to depend on bias voltage for finite embedding admittance. However, this assumption simplifies discussion of the important effects, and yield results that are qualitatively similar to those obtained when the actual LO drive voltage is used. This assumption is used throughout the paper, except when we discuss the physical origin of the effect of the quantum susceptance on the output admittance of the junction.

To illustrate general trends, we consider three sets of imbedding admittances, summarized in the table below.

set	Y_{USB}	Y_{LSB}	Y_{IF}
a	0.020 - 0.018i	0.020 - 0.022i	0.020 + 0.000i
b	0.020 + 0.002i	0.020 - 0.002i	0.020 + 0.000i
c	0.020 + 0.022i	0.020 + 0.018	0.020 + 0.000i

The upper and lower side band embedding susceptances are inductive in set a), nearly zero in set b), and capacitive in set c), as would be the case if the mixer were being operated slightly below the resonant frequency, at the resonant frequency, and slightly above the resonant frequency of the tuning circuit, respectively. The difference between the upper and lower side band embedding admittances is determined by the assumed value of the junction capacitance and the assumed frequency dependance of the inductive tuning element.

The small signal conversion gain and the input and output admittances of the mixer are determined from the small-signal admittance matrix or Y-matrix, which relates currents i_n to voltages v_m at the various sideband frequencies f_n and f_m. Here, $f_m = f_{IF} + mf_{LO}$. The Y-matrix is calculated using the Tucker theory from the dc I-V curve, the dc bias point, and the amplitude of the LO voltage.[2,4]

Mixer Gain

The available mixer gain from the upper sideband frequency to the IF calculated with the Y-matrices calculated using the above assumptions is plotted as a function of dc bias voltage in Fig. 2 for each set of embedding admittances. We should point out two general trends that we will explain. As the imaginary part of the embedding admittance changes from inductive to capacitive, the bias voltage at which the optimum available gain occurs increases from the lower end of the first photon-assisted tunneling step, and the overall magnitude of the gain decreases.

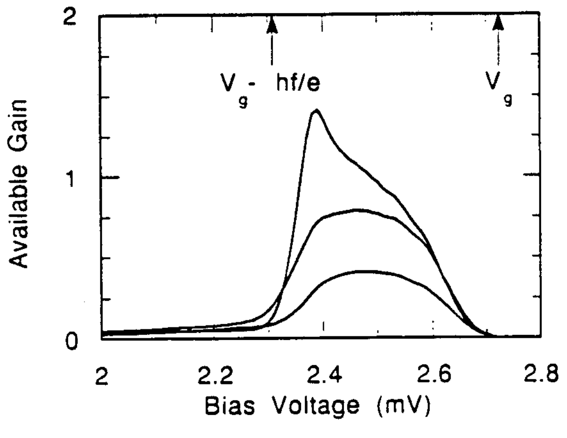

Fig. 2 Available mixer gain from upper side band frequency to the IF plotted as a function of dc bias voltage for each set of embedding admittances. The LO drive voltage is set at 0.4 mV, independent of dc bais voltage.

To understand these trends, we can write the available gain from the USB frequency as

$$L^{-1} = \frac{G_S}{(Y_{11} + Y_S)^2} \, |Y_{01}|^2 \, \frac{4 G_L}{(G_L + G_{OUT})^2} \qquad (1)$$

Here, $Y_s = G_s + iB_s$ is the embedding admittance at the signal frequency, $Y_{11} = \partial i_s/\partial v_s$ and $Y_{01} = \partial i_{IF}/\partial v_s$ are elements of the Y-matrix, G_L is the load conductance, and G_{OUT} is the output conductance of the mixer at the IF frequency. An equivalent circuit is shown in Fig. 3, which shows the signal source with output admittance Y_s, the mixer itself, and the IF circuit represented by the load conductance G_L. The first factor in Eq. 1 can be viewed as characterizing the coupling of the signal to the mixer, the second factor as being responsible for the actual mixing, and the third factor as characterizing the coupling of the IF signal to the load. It appears that the upper side band mixer gain does not depend on the embedding admittance at the lower side band. This is not in fact the case. G_{OUT} depends on the both the upper and lower sideband embedding admittances, but not on the IF load admittance G_L.

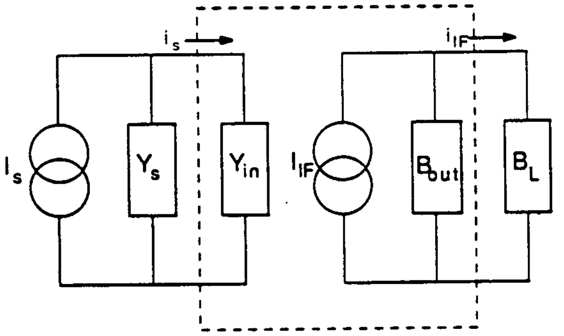

Fig. 3 The equivalent circuit used to evaluate mixer performance. The source is modeled as a current source with output admittance Y_S. The IF port of the mixer is modeled as a current source of magnitude I_{IF} with output conductance G_{OUT}. The IF load has conductance G_L. The region inside the dotted rectangle is the mixer, the region outside is the embedding circuit.

When V_{LO} is independent of bias voltage, and for low IF, Y_{01} is purely real and nearly independent of bias voltage on the first photon-assisted tunneling step. Also, Y_{01} is independent of embedding admittance. Therefore, if the quantum susceptance is to influence the mixer gain, it must do so by its effect on the coupling of the signal in and out of the mixer. We will first discuss the couping of the signal into the mixer at the signal frequency.

To further simplify the discussion, we make the "low IF" approximation. We assume that the dc I-V curve is linear on the voltage scale associated with the IF (hf_{IF}/e). In other words,

$$I_{dc}(V + hf_{IF}/e) - I_{dc}(V - hf_{IF}/e)/(2hf_{IF}) = dI_{dc}(V)/dV \qquad (2)$$

at the dc bias voltage, and at bias voltages nhf_{LO}/e above and below the dc bias voltage. Since an SIS mixer is typically operated near the middle of a photon-assisted tunneling step, this assumption is valid for most SIS mixers. This assumption is made for discussion purposes only, all quantities calculated in this work are calculated without using the low IF approximation.

Bias Voltage Dependence of Y_{11}

First we calculate the value of Y_{11} of the mixer as a function of dc bias voltage. The LO drive voltage V_{LO} is fixed at 0.4 mV as it is for all subsequent calculation in this paper. The real and imaginary parts Y_{11} are plotted in Fig. 4 as a function of bias voltage. The range of voltages from 2.4 to 2.7 mV is where the first

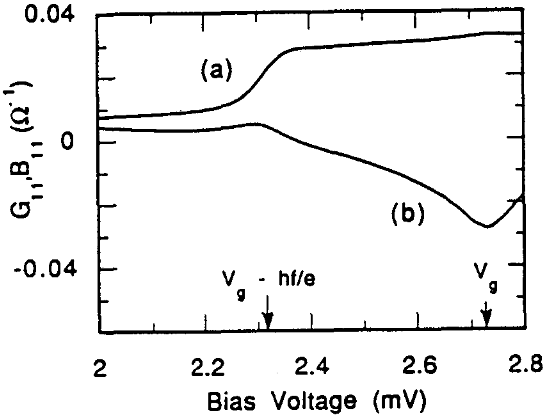

Fig. 4 (a) The real (G_{11}) and (b) imaginary (B_{11}) part of Y_{11} plotted as a function of bias voltage. The LO drive voltage V_{LO} is 0.4 mV. Note that the real part is nearly constant between 2.25 and 2.7 mV, while the imaginary part changes rapidly over this same range of bias voltage.

photon assisted tunneling step occurs for an LO frequency of 100 GHz, and is the region of operation for a typical SIS mixer. Over this range, the real part of Y_{11} is nearly constant, while the imaginary part changes dramatically from capacitive (positive) at 2.4 mV to inductive (negative) at 2.7 mV. Depending on the value of the embedding admittance, this rapid change of the imaginary part can change the bias voltage at which the optimum coupling of the signal to the mixer occurs.

Quantum Susceptance and the Input Coupling

Now that we have calculated the input admittance at the signal frequency, we can substitute it into the first factor in Eq. 1 to examine the coupling of the signal to the mixer. In Fig. 5, we plot the quantity $G_s/|Y_s + Y_{11}|^2$ as a function of bias voltage for each set of imbedding admittances. Between 2.40 and 2.65 mV (on the first photon-assisted tunneling step) the real part of Y_{11} is nearly constant, so any change in the coupling coefficient is due to the large change in the imaginary part as a function of bias voltage. The coupling coefficient should be maximized when the sum of the B_s and imaginary part of Y_{11} is zero. When Y_s is inductive as in admittance set a), the coupling is maximized on the lower bias voltage end of the step, as in Fig 5a. When the Y_s is capacitive, as in admittance set c), the coupling is maximized at the higher bias voltage end of the step, as is shown in Fig 5c. When the Y_s is purely real, neither end of the step is favored.

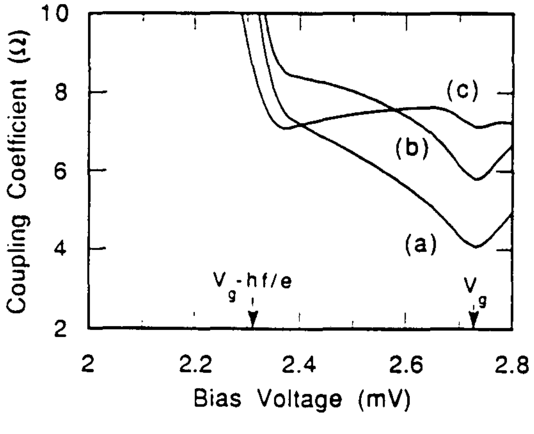

Fig. 5 RF coupling coefficient $G_s/|Y_s + Y_{11}|^2$ plotted as a function of bias voltage, (a), (b), and (c) for admittance sets a, b, and c, respectively.

Bias Voltage Dependence of the Output Admittance

In order to gain physical intuition, we discuss the effect of the quantum susceptance on the output admittance of the mixer from the point of view of the shape of the dc I-V curve with the LO applied. In addition to the assumptions already made, we must assume that the embedding admittances at the upper and lower side bands are equal (double sideband mixer). This is nearly true for our hypothetical mixer because of its relatively low capacitance and the slow change of the inductance of the tuning element with frequency.

Under this assumption, it has been shown that the output admittance of the mixer at the IF is real, and equal to the dynamic conductance of the pumped I-V curve.[4] We have already published a physical explanation for the shape of the pumped I-V curve including the interaction of the quantum susceptance and the embedding admittance,[8,7] but we will summarize it here for completeness.

The dynamic conductance of the pumped I-V curve can be divided into two parts

$$G_D = \frac{dI_{dc}(V_o, V_f)}{dV_o} = \frac{\partial I_{dc}(V_o, V_f)}{\partial V_o} + \frac{d\alpha}{dV_o}\frac{\partial I_{dc}(V_o, V_f)}{\partial \alpha}$$

$$= \sum_{n=-\infty}^{\infty} J_n^2(\alpha)\,\frac{\partial I_{dc}(V_o + nhf/e)}{\partial V_o} + \qquad (3)$$

$$\frac{d\alpha}{dV_o}\frac{\partial}{\partial \alpha}\sum_{n=-\infty}^{\infty} J_n^2(\alpha)\, I_{dc}(V_o + nhf/e)$$

Here, $I_{dc}(V_o, V_f)$ is the dc current of the pumped SIS junction, $I_{dc}(V_o + nhf_{LO}/e)$ is the dc I-V curve of an unpumped SIS evaluated at a bias voltage $V_o + nhf_{LO}/e$, $\alpha = eV_{LO}/hf_{LO}$ is the dimensionless LO voltage, and J_n is a Bessel function of order n.

The first term in Eq. 3 is the dynamic conductance of an I-V curve pumped with constant LO voltage. This is almost always positive unless the unpumped dc I-V curve junction under study has a pronounced super-gap structure induced by the proximity effect. The second term is due to the change in LO pump voltage with dc bias voltage. It can either be positive or negative depending on the embedding admittance.

The left side of the equivalent circuit shown in Fig. 2 can be used to analyze the dependence of V_{LO} on V_o. The large signal input admittance of the junction at the LO frequency is qualitatively similar to the small signal input admittance at the upper sideband frequency shown in Fig. 4. The real part is nearly constant on a photon-assisted tunneling step, and the imaginary part changes rapidly from capacitive to inductive as the dc bias voltage is increased from the low voltage end of the step. If the imbedding admittance is inductive, the inductive embedding susceptance in parallel with the inductive input admittance combine to shunt the LO signal at the high voltage end of the step. At the low voltage end of the step, the capacitive input susceptance cancels the inductive embedding susceptance, and the LO current must flow through the conductive part of the circuit. This leads to a larger value of V_{LO} at the lower voltage end of the step than at the higher voltage end of the step. Thus $d\alpha/dV_o$ is negative, and the dynamic conductance of the pumped I-V curve is reduced. If $d\alpha/dV_o$ is large enough, the dynamic conductance may even become negative. If the embedding admittance is capacitive, the effect is reversed, and the dynamic conductance is increased.

It should be noted that the above argument only applies when the value of the embedding susceptance is comparable to the change in input susceptance with bias voltage. The values of the input susceptance are roughly the same as the normal conductance of the junction for a junction with a moderately sharp current rise at the sum-gap.

In Fig. 6, we plot the real and imaginary parts of the output admittance of the mixer at the IF as functions of bias voltage for the 3 sets of embedding admittances. As discussed above, the imaginary parts are nearly zero for all bias voltages. As the embedding admittance changes from inductive to capacitive, the real part of the admittance on the first photon-assisted tunneling step

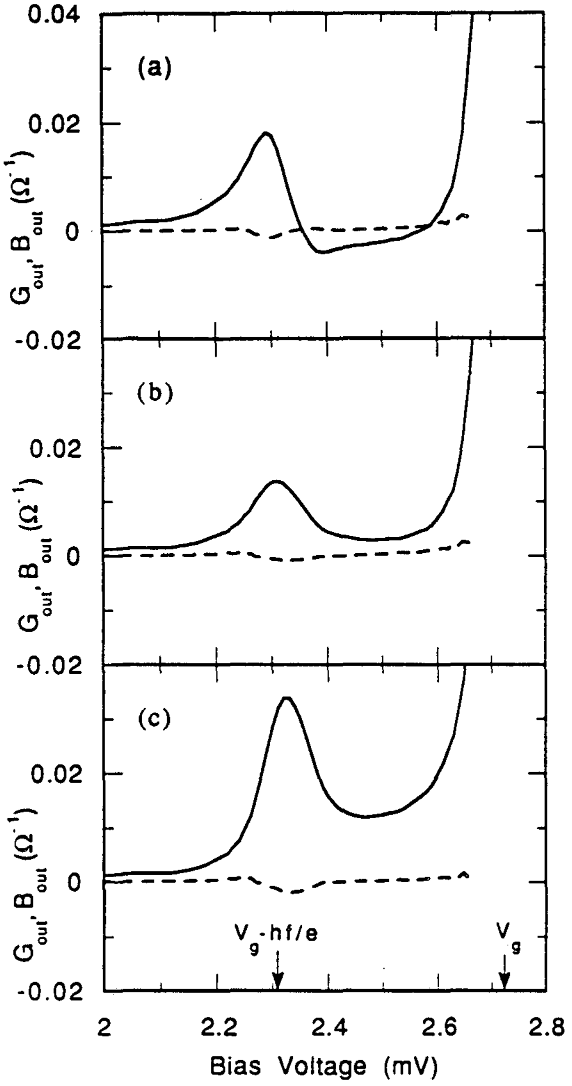

Fig. 6 Real (solid line), and imaginary (dotted line) parts of the IF output impedance of the mixer for admittance sets a, b, and c.

increases from a negative to a positive value. It should be emphasized that these calculations were made without the low-IF, double sideband assumptions that were used to facilitate discussion. If we perform the same calculation without including the quantum susceptance, the output conductance is independent of the RF embedding susceptance on the first photon-assisted tunneling step, as shown in Fig 7.

Quantum Susceptance and IF coupling

Equation 1 can be interpreted as the power coupled to a load conductance G_L by a current source of magnitude

$$\sqrt{8P_{AV}G_S}\ \frac{Y_{01}}{Y_S+Y_{11}} \qquad (4)$$

with an output admittance G_{OUT}. Here P_{AV} is the available power at the signal frequency. As we change the RF embedding admittance from inductive to capacitive, the magnitude of the current source does not change significantly. However, G_{OUT} does change. As G_{OUT} approaches zero, the available power $P_{AV} = I_0^2/2G_{OUT}$ becomes large, and is infinite whenever G_{OUT} is less then zero. Therefore, as the embedding admittance changes from capacitive to inductive, the available gain increases to infinity. Since, at least for the typical case that we study here, the output conductance does not become negative without the presence of the quantum susceptance, we can say that the quantum susceptance is responsible for the infinite available gain for SIS mixers using junctions with I-V curves with moderately sharp current rises at the sum-gap voltage.

Conclusion

In conclusion, we have argued that the main effect the out-of-phase tunneling currents have on the performance of SIS mixers is through the coupling of the radiation in and out of the mixer. By studying a hypothetical case, we have shown that at the signal port, the principal effect is to change the bias voltage at which optimum coupling to the mixer occurs. A more dramatic effect occurs at the IF port, where the quantum susceptance leads to negative values of the output conductance, which causes the available gain to be infinite.

This work was supported in part by the Director, Office of Energy Research, Office of Basic Energy Sciences, Chemical Sciences Division of the U.S. Department of Energy under Contract No. DE-AC03-76-SF00098.

References

1. P. L. Richards and Qing Hu, "Superconducting components for infrared and millimeter-wave receivers," *Proceedings of the IEEE*, vol. 77, 1233-1246, 1989.
2. J. R. Tucker, "Quantum Limited Detection in Tunnel Junction Mixers," *IEEE J. Quantum Electron.*, vol. QE-15, 1234-1258, Nov. 1979.
3. J. R. Tucker, "Predicted Conversion Gain in Superconductor-Insulator-Superconductor Quasiparticle Mixers," *Appl. Phys. Lett.*, 477-479, 15 March 1980.
4. J. R. Tucker and M. J. Feldman, "Quantum Dectection at Millimeter Wavelengths," *Rev. Mod. Phys.*, vol. 57, 1055-1113, Oct. 1985.
5. N. R. Werthamer, "Nonlinear self-coupling of Josephson radiation in superconducting tunnel junctions," *Phys. Rev.*, vol. 147, 255-263, 1966.
6. Qing Hu, C. A. Mears, P. L. Richards, and F. L. Lloyd, "Observation of Nondissipative Quasiparticle Tunnel Currents in Superconducting Tunnel Junctions," *Phys. Rev. Lett.*, vol. 64, 2945-2948, June 1990
7. Qing Hu, C. A. Mears, P. L. Richards, and F. L. Lloyd, "Quantum Susceptance and its effects on the high frequency response of superconducting tunnel junctions," to be published in *Phys. Rev. B*, 1990.
8. C. A. Mears, Qing Hu, and P. L. Richards, "Numerical Simulation on Experimental Data from Planar SIS Mixers with Integrated Tuning Elements," *IEEE Trans. Magn.*, vol MAG-25, 1050-1053, 1989.
9. M. J. Feldman, "Some analytical and intuitive results in the quantum theory of mixing," *J. Appl. Phys.*, vol. 53, 584-592, 1982.
10. M. J. Feldman and D. W. Face, "Image frequency termination of the superconducting quasiparticle mixer," *Jap. Jour. of Appl. Phys.*, vol. 26, 1633-1635, 1987.
11. A. V. Räisänen, D. G. Crété, F. L. Lloyd, and P. L. Richards, "A 100-GHz quasiparticle mixer with 10 dB coupled gain," *IEEE MTT-S Dig.*, 929-930, 1987.
12. Li Xizhi, P. L. Richards, and F. L. Lloyd, "SIS Quasiparticle Mixers with Bow-Tie Antennas," *Int J. Infrared and Millimeter Waves*, vol. 9, 101-133, 1988.
13. Qing Hu, C. A. Mears, P. L. Richards, and F. L. Lloyd, "MM Wave Quasioptical SIS Mixers," *IEEE Trans Magn.* vol. MAG-25, 1380-1383, 1989.

LAWRENCE BERKELEY LABORATORY
UNIVERSITY OF CALIFORNIA
INFORMATION RESOURCES DEPARTMENT
BERKELEY, CALIFORNIA 94720